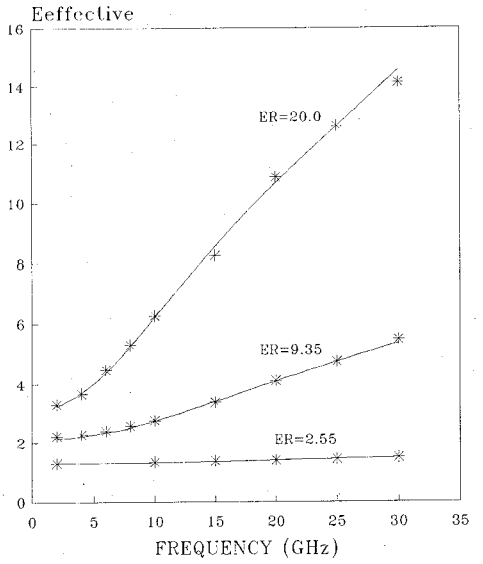

Fig. 4. Effective dielectric constant versus frequency for different dielectric substrates. Solid lines show results obtained with SDA, whereas asterisks are Yamashita's results [2].

narrow strips the number of spectral terms necessary to obtain an accuracy of 0.1% in both ϵ_{eff} and Z_0, is of the order of at least 250 terms for the effective dielectric constant and 350 terms for the characteristic impedance. On the contrary, for wider strips the number of only 150 spectral terms ensures the same order of accuracy (0.1%) for both ϵ_{eff} and Z_0. Now, it is worth noting the behavior of the solution for ϵ_{eff}, which is obtained using the set numbered 1 in Table I. In the case of wide strips it converges to a value that deviates from the reference one by about 0.3%. This behavior states the fact that even at the lower frequencies of the millimeter-wave band the zero order approximation leads to an error in the computation of ϵ_{eff} when wider strips are considered.

Finally, in order to evaluate the accuracy of our analysis and the proper functioning of the computing program, a comparison is made between our results and those found by Yamashita [2] for frequencies up to 30 GHz. It is assumed that the suspended substrate microstrip line is placed in a shielding with outer dimensions $A = 20$ mm and $B = 10$ mm. The strip width is 2 mm, and the dielectric substrate has a thickness of 1 mm. Three different dielectric substrates are considered, that is, three different dielectric constants: $\epsilon_r = 2.55$, $\epsilon_r = 9.35$ and $\epsilon_r = 20$, respectively. The results, as shown in Fig. 4, are obtained using the set of basis functions number 4 in Table I with 350 spectral terms. In the same figure the results obtained by Yamashita [2], who employed the method of non-uniform discretization of integral equations, are also shown. Clearly, a good agreement exists between our results and those reported by Yamashita.

IV. Conclusion

The comparison of various basis functions that can be used in the study of the shielded suspended substrate microstrip lines, and the convergence behavior of their solutions have shown that the longitudinal current component on the strip is essential for an accurate analysis of these lines, especially in the millimeter-wave region. It is concluded that the set of basis functions number 4 in Table I should be used in order to obtain fast and accurate results. However, the sets 3 and 5 may be also used if less accuracy is acceptable.

Acknowledgment

During this research I. P. Polichronakis was holder of an I.K.Y. scholarship and he would like to express his gratitude to I.K.Y.

References

[1] M. H. Arain, "A 94 GHz suspended stripline circulator," in *1984 IEEE MTT-S Int. Microwave Symp. Dig.*, pp. 78–79.
[2] E. Yamashita and K. Atsuki, "Analysis of microstrip-like transmission lines by nonuniform discretization of integral equations," *IEEE Trans. Microwave Theory Tech.*, vol. MTT-24, pp. 195–200, 1976.
[3] R. Crampagne, M. Ahmadpanah, and J. L. Guiraud, "A simple method for determining the Green's function for a large class of MIC lines having multilayered dielectric structures," *IEEE Trans. Microwave Theory Tech.*, vol. MTT-26, pp. 82–87, Feb. 1978.
[4] R. S. Thomar and P. Barchia, "Suspended and inverted microstrip design," *Microwave J.*, pp. 173–178, Mar. 1986.
[5] T. Itoh, "Spectral domain immitance approach for dispersion characteristics of generalized printed transmission lines," *IEEE Trans. Microwave Theory Tech.*, vol. MTT-28, pp. 733–736, July 1980.
[6] J. B. Knorr and A. Tufekcioglu, "Spectral domain calculation of microstrip characteristic impedance," *IEEE Trans. Microwave Theory Tech.*, vol. MTT-23, pp. 725–728, Sept. 1975.
[7] T. Itoh and R. Mittra, "A technique for computing dispersion characteristics of shielded microstrip lines," *IEEE Trans. Microwave Theory Tech.*, vol. MTT-22, pp. 896–898, Feb. 1974.
[8] R. H. Jansen, "High speed computation of single and coupled microstrip parameters including dispersion, high-order modes, loss and finite strip thickness," *IEEE Trans. Microwave Theory Tech.*, vol. MTT-26, pp. 75–82, Feb. 1978.
[9] T. Leung and C. A. Valanis, "Pulse dispersion distortion in open and shielded microstrips using the spectral-domain method," *IEEE Trans. Microwave Theory Tech.*, vol. 36, pp. 1223–1226, July 1988.
[10] E. J. Delinger, "A frequency depended solution for microstrip transmission lines," *IEEE Trans. Microwave Theory Tech.*, vol. MTT-19, pp. 30–39, Jan. 1971.
[11] M. Kobayashi, "Longitudinal and transverse current distributions on microstriplines and their closed-form expression," *IEEE Trans. Microwave Theory Tech.*, vol. MTT-33, pp. 784–788, Sept. 1985.
[12] L. P. Schmidt and T. Itoh, "Spectral domain analysis of dominant and higher order modes in fin-lines," *IEEE Trans. Microwave Theory Tech.*, vol. MTT-28, pp. 981–985, Sept. 1980.
[13] M. Kobayashi and T. Iijima, "Frequency-dependent characteristics of current distributions on microstrip lines," *IEEE Trans. Microwave Theory Tech.*, vol. 37, pp. 799–801, Apr. 1989.

18–42 GHz Experimental Verification of Microstrip Coupler and Open End Capacitance Models

Andrew J. Slobodnik, Jr., Richard T. Webster, and George A. Roberts

***Abstract*—A cavity resonance technique is used to experimentally verify microstrip coupler and open end capacitance models over the frequency range 18–42 GHz. In addition, these results are confirmed using an alternative version of the technique which directly determines**

Manuscript received June 24, 1991; revised November 7, 1991.

The authors are with the Electromagnetics and Reliability Directorate, Department of the Air Force, Rome Laboratory (AFSC), Hanscom Air Force Base, MA 01731-5000.

IEEE Log Number 9105702.

open end discontinuity capacitance. In the second case knowledge of substrate dielectric constant is not required and the method also yields microstrip relative effective dielectric constant.

I. Introduction

The need for accurate microstrip discontinuity models for the design of monolithic microwave and millimeter wave integrated circuits has motivated considerable work in this area [1]–[8]. Much of this effort has been theoretical in nature. The objective of the present paper is to experimentally verify the model for microstrip open end [9], [10] fringing capacitance over the frequency range 18–42 GHz. This paper therefore complements the lower frequency (8–12 GHz) work of Uwano [11]. Since a microstrip coupler [12], [13] is used as part of the measurement technique, verification of this model is also obtained.

II. Cavity Technique

Precise measurement of microstrip discontinuities is difficult. To determine what is typically a 2% effect to within 20% accuracy requires an overall precision of 0.4%. Since frequency can be very accurately measured, a cavity resonance technique [11], [14], [15] provides a good approach. Therefore a number of cavities of the type illustrated in Fig. 1 were constructed. Resonance characteristics were measured using a calibrated automatic network analyzer and curve fitting to the data was performed to obtain f_{exp} to within 0.005%. These experimental resonant frequencies were compared to the predictions of Touchstone® [16] using their models for microstrip, parallel coupled lines and open end capacitance. Results for $(f_{mod} - f_{exp})/f_{mod} = \Delta f/f_{mod}$ using both impedance dispersion options [17], [18] are shown in Fig. 2. Agreement between theory and experiment is good thus confirming the models to within the level of uncertainty. The measure of uncertainty illustrated in Fig. 2 is $\Delta f^{rss}_{err}/f_{mod} = (\Sigma_{i=1}^{4}(\Delta f^{i}_{err})^2)^{1/2}/f_{mod}$. The four major sources of error are included: accuracy of dispersion in the relative effective dielectric constant used for the microstrip model [19], accuracy of the odd- and even-mode effective dielectric constants used for the coupler model [13], uncertainty in substrate ϵ_r [14], [20], and accuracy of cavity length as measured by laser interferometer. To illustrate the influence of open end capacitance on the resonant frequencies, the Touchstone® (Getsinger) results of Fig. 2 are repeated in Fig. 3 which also includes results for the model with fringing capacitance set to zero. Clearly open end discontinuity capacitance is a measurable effect. Average dimensions corresponding to Figs. 2 and 3 are line width $W = 0.218$ mm, coupler gap $S = 0.313$ mm, coupler length $l_c = 1.394$ mm for $f_o < 30$ GHz and 0.784 mm for $f_o > 30$ GHz. Overall cavity length, $l_{ML} + l_c + l_{MR}$, is varied to achieve the different center frequencies. Quantities are defined in Fig. 4(a) and (b). Alumina substrate average thickness is 0.272 mm with a cover height of 1.524 mm. Nominal metallization is 4.1 μm gold.

III. Multiple Cavity Technique

The previous analysis used a dielectric constant value of $\epsilon_r = 9.9$ which is within the accepted range [14], [20] for 99.6% alumina. The good agreement between theory and experiment indicates that this ϵ_r value is reasonable for the particular substrates used. However, an alternative version of the cavity resonance technique which does not depend on prior knowledge of ϵ_r would be useful to confirm the previous results. Such a technique was devised and is described below.

For the simple cavity shown in Fig. 4(a) there are three primary quantities that determine the frequency. These are the sought after open end capacitance, C_E, the relative effective dielectric constant, $\epsilon^{M}_{reff}(f_o)$, and the length, l. The effect of the loosely coupled feed

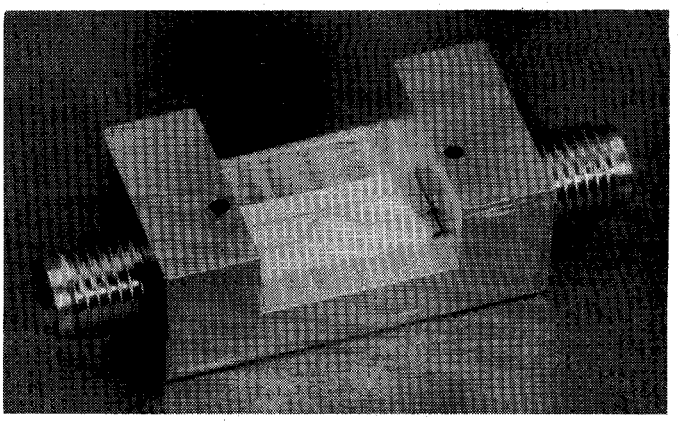

Fig. 1. Photograph of typical open end cavity in test package. Cavity itself consists of two outer sections of microstrip plus an inner section of microstrip coupled lines.

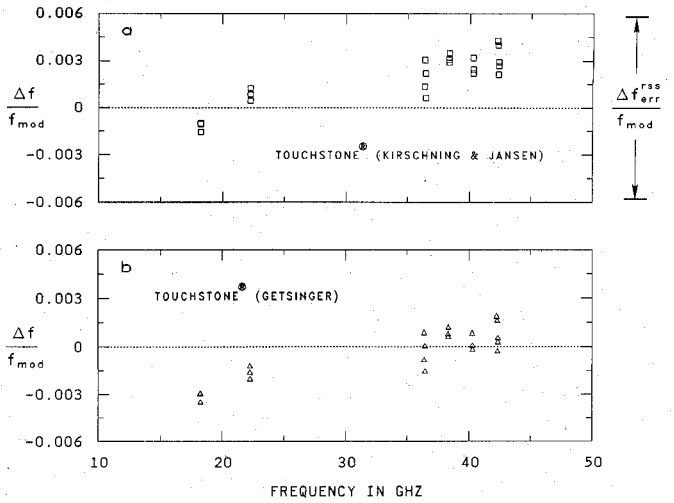

Fig. 2. Comparison of open end cavity resonant frequency theory and experiment using the quantity $(f_{mod} - f_{exp})/f_{mod} \cdot f_{mod}$ computed by Touchstone® using indicated impedance dispersion option. Uncertainity interval, $\Delta f^{rss}_{err}/f_{mod}$, corresponds to root sum of squares.

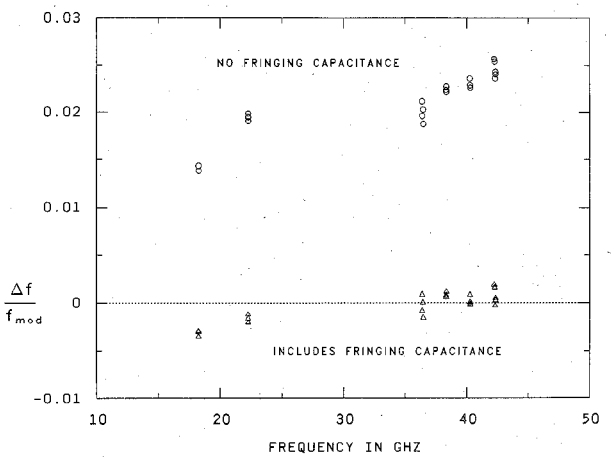

Fig. 3. Comparison of open end cavity resonant frequency theory and experiment using the quantity $(f_{mod} - f_{exp})/f_{mod} \cdot f_{mod}$ computed by Touchstone® (Getsinger) both with and without open end fringing capacitance.

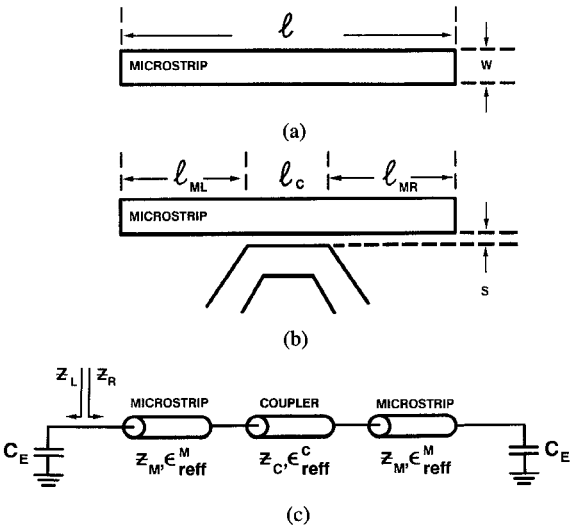

Fig. 4. (a) Schematic representation of simple microstrip cavity. (b) Cavity with coupler as used throughout this paper. (c) Transmission line equivalent circuit of cavity with coupler.

line shown in Fig. 4(b) can be represented by using a different relative effective dielectric constant, $\epsilon^{c}_{reff}(f_o)$, in this region. The transmission line equivalent circuit is shown in Fig. 4(c).

The main feature of the alternative technique is that multiple cavities at slightly different frequencies f_i are used. Relative dispersion between these frequencies, although in essence a second order effect, must be accounted for. While dispersion correction to the average frequency f_k could be accomplished experimentally [21], theory [15], [19], [22], [23] was used according to (7) since the relative correction is less demanding of the theory than a requirement for an absolute value. In similar manner, impedance (a second order effect with respect to resonant frequency) was taken directly from theory [17], $Z^{i}_{M,C} = Z^{TH}_{M}(f_i)$. $\epsilon^{M}_{reff}(f_k)$ and $\epsilon^{C}_{reff}(f_k)$ become unknowns along with C_E. In addition, it was found that improved solutions could be obtained by using four cavities, two open and two shorted. This introduces a fourth unknown, via inductance to ground, and results in four transmission line resonance equations (1) to be solved numerically for the unknowns. These resonance equations represent the condition for natural oscillation [24] in a transmission line system. That is, the sum of reactances looking to the left and to the right at any reference plane must equal zero. Our particular reference plane is shown in Fig. 4(c).

$$\text{Im}\,[Z_L + Z_R] = \text{Im}\left[Z^{i}_{E} + Z^{i}_{M}\left(\frac{1 + \Gamma_{2i}e^{2\gamma^{i}_{M}l^{i}_{ML}}}{1 - \Gamma_{2i}e^{2\gamma^{i}_{M}l^{i}_{ML}}}\right)\right] = 0$$

$$i = 1, 4 \tag{1}$$

where

$$\Gamma_{2i} = \frac{Z^{i}_{2} - Z^{i}_{M}}{Z^{i}_{2} + Z^{i}_{M}}, \quad Z^{i}_{2} = Z^{i}_{c}\left(\frac{1 + \Gamma_{1i}e^{2\gamma^{i}_{c}l^{i}_{c}}}{1 - \Gamma_{1i}e^{2\gamma^{i}_{c}l^{i}_{c}}}\right) \tag{2}$$

$$\Gamma_{1i} = \frac{Z^{i}_{1} - Z^{i}_{c}}{Z^{i}_{1} + Z^{i}_{c}}, \quad Z^{i}_{1} = Z^{i}_{M}\left(\frac{1 + \Gamma_{Ei}e^{2\gamma^{i}_{M}l^{i}_{MR}}}{1 - \Gamma_{Ei}e^{2\gamma^{i}_{M}l^{i}_{MR}}}\right) \tag{3}$$

$$\Gamma_{Ei} = \frac{Z^{i}_{E} - Z^{i}_{M}}{Z^{i}_{E} + Z^{i}_{M}} \tag{4}$$

$$\gamma^{i}_{M,C} = \frac{j2\pi f_i\sqrt{\epsilon^{M,C}_{reff}(f_i)}}{v_{light}} \tag{5}$$

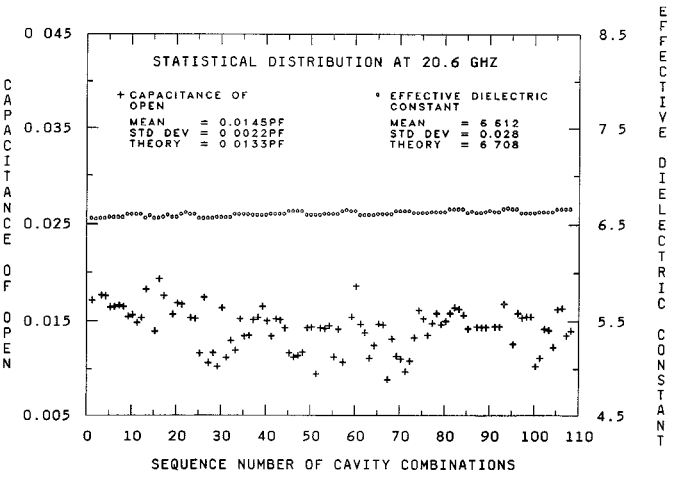

Fig. 5. Results of statistical analysis of 13 cavities with capacitance in pF. Resonant frequencies were in the range 18.24–22.73 GHz. Theoretical values are from Kirschning, Jansen, and Koster [9], [19].

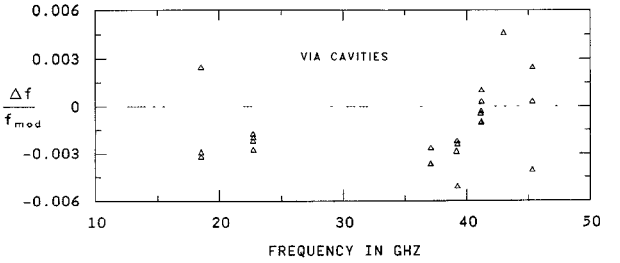

Fig. 6. Comparison of via cavity resonant frequency theory and experiment using the quantity $(f_{mod} - f_{exp})/f_{mod}$. f_{mod} computed by Touchstone® (Getsinger) with inductor from multiple cavity technique representing vias at both ends.

$$Z^{i}_{E} = \frac{1}{j2\pi f_i C_E} \qquad i = 1, 3$$

$$Z^{i}_{E} = j2\pi f_i L_E \qquad i = 2, 4 \tag{6}$$

and

$$\epsilon^{M,C}_{reff}(f_i) = \epsilon^{M,C}_{reff}(f_k)\frac{\epsilon^{MTH}_{reff}(f_i)}{\epsilon^{MTH}_{reff}(f_k)}. \tag{7}$$

IV. Analysis

Results from thirteen (18.24–22.73 GHz) cavities were analyzed by solving for the four unknowns for 108 combinations of four cavities. After elimination of eight obviously bad cases, the statistical results for C_E and ϵ^{M}_{reff} are as shown in Fig. 5. The comparison of theory and experiment also provided in Fig. 5 supports the earlier conclusion of model accuracy.

In addition to values for C_E and ϵ^{M}_{reff}, 0.044 nH nominal inductance to ground for an average 0.325 mm diameter via hole was also determined. This inductance value can be used with the previous basic cavity technique as a final check for self consistency. The results shown in Fig. 6 further confirm model correctness. Average dimensions corresponding to Fig. 6 are similar to those provided for Figs. 2 and 3.

V. Summary

Microstrip, coupler and open end capacitance models used in Touchstone® have been checked experimentally over the frequency

range 18–42 GHz. Center frequencies of open end cavities using 0.218 mm wide lines on 0.272 mm thick alumina can be predicted to within 0.45%. In addition, a four cavity technique for measuring open end discontinuity capacitance and $\epsilon_{reff}^{M}(f)$ has been described.

References

[1] R. H. Jansen and L. Wiemer, "Full wave theory based development of MM-wave circuit models for microstrip open end, gap, step, bend and tee," in *1989 IEEE MTT-S Int. Microwave Symp. Dig.*, pp. 779–782.

[2] X. Zhang and K. K. Mei, "Time-domain finite difference approach to the calculation of the frequency-dependent characteristics of microstrip discontinuities," *IEEE Trans. Microwave Theory Tech.*, vol. 36, pp. 1775–1787, Dec. 1988.

[3] L. P. Dunleavy and P. B. Katehi, "Shielding effects in microstrip discontinuities," *IEEE Trans. Microwave Theory Tech.*, vol. 36, pp. 1767–1773, Dec. 1988.

[4] P. B. Katehi and N. G. Alexopoulos, "Frequency-dependent characteristics of microstrip discontinuities in millimeter-wave integrated circuits," *IEEE Trans. Microwave Theory Tech.*, vol. MTT-33, pp. 1029–1035, Oct. 1985.

[5] R. W. Jackson and D. M. Pozar, "Full-wave analysis of microstrip open-end and gap discontinuities," *IEEE Trans. Microwave Theory Tech.*, vol. MTT-33, pp. 1036–1042, Oct. 1985.

[6] J. X. Zheng and D. C. Chang, "Numerical modeling of chamfered bends and other microstrip junctions of general shape in MMIC's," in *1990 IEEE MTT-S Int. Microwave Symp. Dig.*, pp. 709–712.

[7] J. McLean, H. Ling, and T. Itoh, "Full wave modeling of electrically wide microstrip open end discontinuities via a deterministic spectral domain method," in *1990 IEEE MTT-S Int. Microwave Symp. Dig.*, pp. 1155–1158.

[8] T. Uwano, "Characterization of microstrip open end in the structure of a parallel-coupled stripline resonator filter," *IEEE Trans. Microwave Theory Tech.*, vol. 39, pp. 595–600, Mar. 1991.

[9] M. Kirschning, R. H. Jansen, and N. H. L. Koster, "Accurate model for open end effect of microstrip lines," *Electron. Lett.*, vol. 17, pp. 123–125, Feb. 1981.

[10] R. H. Jansen and N. H. L. Koster, "Accurate results on the end effect of single and coupled microstrip lines for use in microwave circuit design," *AEU*, vol. 34, pp. 453–459, 1980.

[11] T. Uwano, "Accurate characterization of microstrip resonator open end with new current expression in spectral-domain approach," *IEEE Trans. Microwave Theory Tech.*, vol. 37, pp. 630–633, Mar. 1989.

[12] R. Garg and I. J. Bahl, "Characteristics of coupled microstriplines," *IEEE Trans. Microwave Theory Tech.*, vol. MTT-27, pp. 700–705, July 1979.

[13] M. Kirschning and R. H. Jansen, "Accurate wide-range design equations for the frequency-dependent characteristic of parallel coupled microstrip lines," *IEEE Trans. Microwave Theory Tech.*, vol. MTT-32, pp. 83–90, Jan. 1984.

[14] T. C. Edwards, *Foundations for Microstrip Circuit Design*. New York: Wiley, 1981.

[15] R. A. York and R. C. Comton, "Experimental evaluation of existing CAD models for microstrip dispersion," *IEEE Trans. Microwave Theory Tech.*, vol. 38, pp. 327–328, Mar. 1990.

[16] Touchstone®, a software simulator for linear microwave and RF circuits, is a product of EEsof®, Westlake, Village, CA 91362. The microstrip line, microstrip line including open end effect, and microstrip coupled lines elements were modeled using algorithms referenced in the EEsof® Touchstone® 2.1 Element Catalog, pp. LEL-87 to LEL-131 and HOW-3.

[17] R. H. Jansen and M. Kirschning, "Arguments and an accurate model for the power-current formulation of microstrip characteristic impedance," *AEU*, vol. 37, pp. 108–112, 1983.

[18] W. J. Getsinger, "Measurement and modeling of the apparent characteristic impedance of microstrip," *IEEE Trans. Microwave Theory Tech.*, vol. MTT-31, pp. 624–632, Aug. 1983.

[19] M. Kirschning and R. H. Jansen, "Accurate model for effective dielectric constant of microstrip with validity up to millimetre wave frequencies," *Electron. Lett.*, vol. 18, pp. 272–273, Mar. 1982.

[20] T. S. Laverghetta, *Microwave Materials and Fabrication Techniques*. Norwood, MA: Artech House, 1984.

[21] H. J. Finlay, R. H. Jansen, J. A. Jenkins, and I. G. Eddison, "Accurate characterization and modeling of transmission lines for GaAs MMIC's," *IEEE Trans. Microwave Theory Tech.*, vol. 36, pp. 961–967, June 1988.

[22] M. Kobayashi, "A dispersion formula satisfying recent requirements in microstrip CAD," *IEEE Trans. Microwave Theory Tech.*, vol. 36, pp. 1246–1250, Aug. 1988.

[23] H. A. Atwater, "Test of microstrip dispersion formulas," *IEEE Trans. Microwave Theory Tech.*, vol. 36, pp. 619–621, Mar. 1988.

[24] R. B. Adler, L. J. Chu and R. M. Fano, *Electromagnetic Energy Transmission and Radiation*. New York: Wiley, 1960.

Scattering at an Offset Circular Hole in a Rectangular Waveguide

C. Sabatier

***Abstract*—A solution is given for the problem of scattering at an offset circular to rectangular junction and at a thick diaphragm, with an offset circular aperture, in a rectangular waveguide. The method used, is mode matching for computing one discontinuity. The difficulty arising from the fact that the eigenmodes of the two waveguides are known in different coordinate systems is overcome by simple transformation for the evaluation of overlap integral between the eigenmodes of each waveguide. Experimental results validate this method.**

Introduction

Waveguide diaphragms with circular apertures are frequently used as matching elements in microwave circuits (cavity filters, waveguide to cavity coupling, etc). While centered holes have been investigated by many authors [1]–[3], the case of offset holes has not been addressed to our knowledge.

The discontinuity, presented Fig. 1, is investigated with the method of field expansion into eigenmodes [4], where the three types of overlap integrals are Vhh (TE modes in the two waveguides), Vee (TM modes in the two waveguides), Veh (TE modes in the first waveguide, TM modes in the second). The fourth overlap integral between TM modes in the first waveguide and TE modes in the second is zero [5].

The field expansion is performed on all TE and TM modes in the two waveguides because there is no symmetry in this problem.

Analysis

Since the common section between the two waveguides is circular ($b \geqq 2R$), the three overlap integrals have been computed in the first coordinate system noted O_1 in polar units (r_1, θ_1). Thus, all of the electric fields of the two waveguides must be written in this system. In fact, we write all fields in Cartesian units (x_1, y_1) and we take the Jacobian when we compute the different overlap integrals. For this reason, all field expressions given below are written in function of r_1 and θ_1, even in the Cartesian coordinate system. This method was given in [3] for a centered hole.

Manuscript received April 18, 1991; revised October 10, 1991.

The author is with the Centre National d'Etudes des Telecommunications, Fort de la Tete de Chien, 06320 La Turbie, France.

IEEE Log Number 9105445.